HEFAT2012
9th International Conference on Heat Transfer, Fluid Mechanics and Thermodynamics
16 – 18 July 2012
Malta

BUOYANCY DROP HYSTERESIS IN A TWO-DIMENSIONAL COUNTERCURRENT LAMINAR OPPOSING MIXED CONVECTION SYSTEM

Martínez-Suástegui L.[a]* Treviño C.[b] and Cajas J.C.[c]
*Author for correspondence
[a]ESIME Azcapotzalco, Instituto Politécnico Nacional, Avenida de las Granjas No. 682, Colonia Santa Catarina, Delegación Azcapotzalco, México, Distrito Federal 02250, Mexico,
E-mail: martinezlorenzo@gmail.com

[b]UMDI, Facultad de Ciencias, Universidad Nacional Autónoma de México, Sisal, Yucatán, Mexico,
E-mail: ctrev@servidor.unam.mx

[c]Facultad de Ciencias, Universidad Nacional Autónoma de México, México, Distrito Federal 04150, Mexico,
E-mail: jc.cajas@gmail.com

ABSTRACT

A laminar, two-dimensional and opposing mixed convection flow confined inside a vertical channel of finite length with adiabatic walls and discrete and isothermal heat sources has been studied numerically by solving the unsteady two-dimensional Navier-Stokes and energy equations. The dynamical behavior of the system is influence by geometrical parameters and three nondimensional parameters: the Reynolds, Richardson, and Prandtl numbers. Results show that for a fixed value of the Reynolds number, if the Richardson number is increased and then decreased along the same path, hysteresis is noted. To understand the principles of this hysteresis behavior, the dynamical properties of the system are analyzed in detail. Numerical predictions of the velocity and temperature fields show that the descending step size does not change the size of the hysteresis effect.

INTRODUCTION

The response of internal forced flow to opposing buoyancy forces is important for understanding heat transfer dynamics due to its relevance in thermal problems related to the cooling of modern electronic equipment, design of compact heat exchangers and solar energy collectors [1-4]. The complexity of gravity driven flows subjected to differential heat sources has been extensively studied in the past. Although multiple studies for laminar opposing mixed convection flows are available in the literature [5-8], most of them focus on studying flow reversion, vortex generation, and the resultant flow and heat transfer characteristics. However, relatively fewer studies deal with the investigation of the self-oscillatory characteristics of Navier-Stokes-type systems in mixed convection [9-12].

Recently, transient laminar flow opposing mixed convection in a vertical channel of finite length subjected to isothermal and discrete heat inputs was studied numerically by solving the unsteady two-dimensional Navier-Stokes and energy equations for the case of symmetrical heating [13]. Results show that with increase in the buoyancy parameter, for a fixed Reynolds number, the system undergoes several transitions and exhibits states of asymmetrical steady-state (symmetry-breaking bifurcation), local vortex oscillation (Hopf bifurcation), global relaxation oscillation (gluing bifurcation), and later chaos. Although it is well known that countercurrent mixed convection systems support multiple dynamical states depending on the value of buoyancy forcing, hysteresis appears not to have been measured or computed for these nonlinear dynamical systems. Nevertheless, the important role of hysteresis has been observed and is well established for a long time [14-16]. Because hysteresis represents a non-trivial impediment to optimizing compact heat exchanger design and cooling of modern electronic equipment, it is desirable to identify conditions such that multiple dynamical states cannot occur. To achieve this goal, the control of these systems requires knowledge of the flow structure and in particular of the conditions for stability and transition to different states.

In this paper, numerical predictions are carried out to examine the changes in the dynamical state of a countercurrent gravity driven mixed convection system when increasing and subsequently decreasing the value of the buoyancy parameter. From the numerical simulations, buoyancy drop hysteresis is observed, such that the transition between different dynamical states proceeds along different paths depending upon the flow's time history. This work deals with quantifying and describing

the hysteretic behaviour of the aforementioned system by using global parameters that describe the final dynamical state reached by the system. In addition, the conditions for the occurrence of a subcritical bifurcation are determined numerically.

NOMENCLATURE

g	[m/s^2]	Magnitude of the gravitational acceleration
Gr	[-]	Grashof number based on the channel width, $Gr = g\beta(T_w-T_0)h^3/\nu^2$
h	[m]	Channel width (characteristic length)
l	[-]	Nondimensional length of the channel, $l=l_1+l_2+l_3$
l_1^*	[m]	Length from the channel inlet to the heated plate/plates
l_1	[-]	$l_1= l_1^*/h$
l_2^*	[m]	Length of the heated plate/plates
l_2	[-]	$l_2= l_2^*/h$
l_3^*	[m]	Length from the heated plate/plates to the channel outlet
l_3	[-]	$l_3= l_3^*/h$
Nu	[-]	Nusselt number
$\overline{Nu}$	[-]	Average Nusselt number
Pe	[-]	Peclet number, U_0h/α
Pr	[-]	Prandtl number, ν/α
q	[W/m^2]	Heat flux per unit area on the heated plate/plates
Re	[-]	Reynolds number based on the channel width, $Re= U_0h/\nu$
Ri	[-]	Richardson number based on the channel width, $Ri=Gr/Re^2$
T	[K]	Temperature
T_0	[K]	Fluid temperature at the channel inlet
T_w	[K]	Temperature of the heated plate/plates
U	[-]	Longitudinal nondimensional velocity, u/u_0
u_0	[m/s]	Fluid velocity at the channel inlet
u,v	[m/s]	Longitudinal and transversal velocity components, respectively
V	[-]	Transversal nondimensional velocity, v/u_0
x,y,z	[m]	Cartesian rectangular coordinates
X	[-]	Nondimensional longitudinal coordinate, $X = x/h$
Y	[-]	Nondimensional transverse coordinate, $Y = y/h$

Special characters

α	[m^2/s]	Thermal diffusivity
β	[K^{-1}]	Thermal volumetric expansion coefficient
λ	[W/mK]	Coefficient of thermal conductivity
ν	[m^2/s]	Kinematic viscosity
ρ_0	[kg/m^3]	Density for $T = T_0$
θ	[-]	Nondimensional temperature
τ	[-]	Nondimensional time

GOVERNING EQUATIONS

The schematic view of the geometry considered, which consists of an unsteady Newtonian, two-dimensional, laminar downflow at the entrance of a vertical duct with finite isothermal heat sources located at both walls is shown in Figure 1. The channel walls are separated by a distance h and axial distances from the entrance section are measured by the x coordinate (positive downward), while transverse distances are measured by y ($y = 0$ at the left wall). The heat sources of length l_2 are located at $x = l_1$ with uniform wall temperature T_w, where $T_w > T_0$. All other surfaces of the channel walls are assumed adiabatic. The forced flow is driven by gravitational force acting vertically downward, entering the duct at ambient temperature T_0. Flow rectifiers are placed at the channel entrance and exit, thus producing a parallel flow at $x = 0$ and $x = l_1 + l_2 + l_3$ with a flat velocity distribution at the channel entrance u_0. The viscous dissipation in the energy equation is neglected and the thermophysical properties of the fluid are assumed to be constant except for the density in the buoyancy term, which is treated according to the Boussinesq approximation.

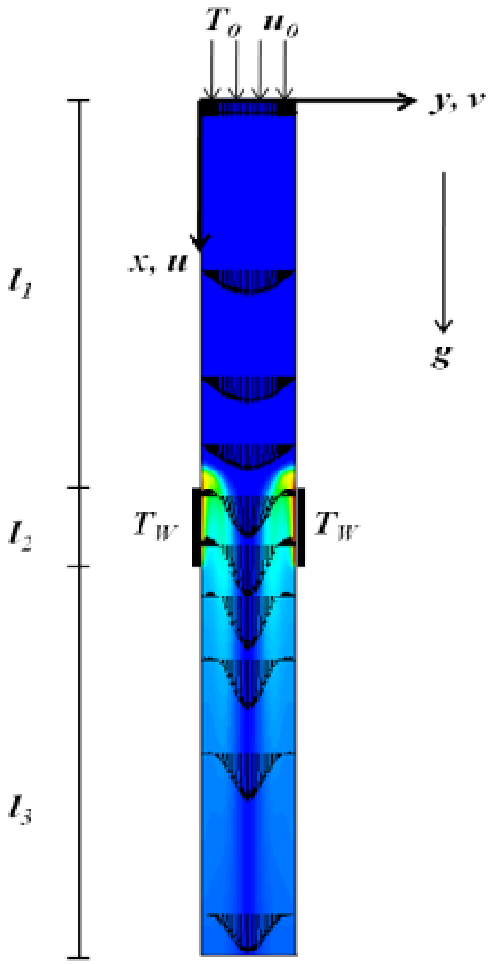

Figure 1 Schematic diagram of the flow and heat transfer problem.

The flow is described by the nondimensional two-dimensional continuity, Navier-Stokes, and energy equations,

$$\frac{\partial U}{\partial X}+\frac{\partial V}{\partial Y}=0 \tag{1}$$

$$\frac{\partial U}{\partial \tau}+U\frac{\partial U}{\partial X}+V\frac{\partial U}{\partial Y}=-\frac{\partial P}{\partial X}+\frac{1}{\mathrm{Re}}\left(\frac{\partial^2 U}{\partial X^2}+\frac{\partial^2 U}{\partial Y^2}\right)-H(\tau)Ri\theta \tag{2}$$

$$\frac{\partial V}{\partial \tau}+U\frac{\partial V}{\partial X}+V\frac{\partial V}{\partial Y}=-\frac{\partial P}{\partial Y}+\frac{1}{\mathrm{Re}}\left(\frac{\partial^2 V}{\partial X^2}+\frac{\partial^2 V}{\partial Y^2}\right) \tag{3}$$

$$\frac{\partial \theta}{\partial \tau}+U\frac{\partial \theta}{\partial X}+V\frac{\partial \theta}{\partial Y}=\frac{1}{Pe}\left(\frac{\partial^2 \theta}{\partial X^2}+\frac{\partial^2 \theta}{\partial Y^2}\right) \tag{4}$$

where U and V are the nondimensional longitudinal and transversal velocity components, respectively, and P and θ are the nondimensional pressure and temperature, respectively. In equations (1) – (4), the velocity components are scaled with the inflow velocity u_0, $U = u/u_0$ and $V = V/u_0$; the longitudinal and

transversal coordinates are scaled with the channel width h, $X = x/h$ and $Y = y/h$; the time is scaled with the residence time h/u_0, $\tau = t\,u_0/h$; the temperature is normalized as $\theta = (T-T_0)/(T_W-T_0)$; and the relative pressure is scaled with the dynamic pressure $\rho_0 u_0^2$, $P = (p - p_0 - \rho_0 g x)/\rho_0 u_0^2$. $H(\tau)$ in equation (2) corresponds to the Heaviside step function, since the assumed initial condition corresponds to the downward flow without buoyancy. Equations (1) – (4) are to be solved with the following boundary conditions:

$$
\begin{aligned}
&U = V = 0, \quad \text{at} \quad Y = 0,1 \\
&P = U - 1 = V = 0, \quad \text{at} \quad X = 0 \\
&V = \frac{\partial U}{\partial X} = 0, \quad \text{at} \quad X = L = L_1 + L_2 + L_3 \\
&\theta = 1, \quad \text{at} \quad Y = 0,1 \quad \text{for} \quad L_1 \le X \le L_1 + L_2 \\
&\frac{\partial \theta}{\partial Y} = 0, \quad \text{at} \quad L_1 > X > L_1 + L_2, \text{ and} \quad Y = 0,1 \\
&\frac{\partial \theta}{\partial X} = 0, \quad \text{at} \quad X = L_1 + L_2 + L_3
\end{aligned}
\tag{5}
$$

Once the nondimensional velocity components U, V, and the nondimensional temperature field is known, the rate of heat flux from each heated slab can be obtained in nondimensional form with the local Nusselt number. The local Nusselt numbers on the left and right heat sources can be evaluated from the equations

$$
Nu_L(X,\tau) = \frac{q(x,t)h}{(T_w - T_0)\lambda} = -\left.\frac{\partial \theta}{\partial Y}\right|_{Y=0}, \quad \text{for} \quad L_1 \le X \le L_1 + L_2 \tag{6}
$$

$$
Nu_R(X,\tau) = \frac{q(x,t)h}{(T_w - T_0)\lambda} = \left.\frac{\partial \theta}{\partial Y}\right|_{Y=1}, \quad \text{for} \quad L_1 \le X \le L_1 + L_2 \tag{7}
$$

where λ is the thermal conductivity of the fluid. The space averaged Nusselt number is then computed by integrating the local Nusselt number along each plate.

$$
\overline{Nu}(\tau) = \frac{1}{L_2}\int_{L_1}^{L_1+L_2} Nu(X,\tau)\,dX. \tag{8}
$$

The position of the recirculation bubbles (vortices) that are generated due to flow reversion close to the heated slabs is represented by a stagnation point at $X=X_s(\tau)$, defined by the maximum value of X, where the longitudinal velocity component is non-negative in the vortex region. It is to be noticed that this point is not a true stagnation point, because the transverse velocity component does not vanish at this point.

The dynamical properties of the system are described using the time evolution for the vortices' upper positions (stagnation points) and the overall Nusselt number.

NUMERICAL SOLUTION PROCEDURE

The dimensionless coordinates were transformed using a non-uniform staggered grid system. Due to the large velocity and temperature gradients, the non-uniform mesh with 121 x 51 grid points has the highest grid density near the channel walls and close to the heated slabs. Information about the grid and time-step sensitivities are given in detail in [17] and are not repeated herein. All calculations were performed using water (Pr = 7) as the cooling agent. In all of the cases studied, numerical runs are carried out employing a computational domain with l = 12. The non-dimensional length of the heated slab/slabs is $l_2 = 1$, and the length of the extended domains so that the obtained solution is independent of their sizes is l_1 = 5.5 and l_3 = 5.5. The time step $\Delta\tau$ was set at 5 x 10^{-4}, since a smaller time step had no significant influence on the results. In order to reproduce the system dynamical response and avoid large induction times, the buoyancy parameter is modified by introducing a temporal asymmetric artificial perturbation term. The modified Richardson number is

$$
Ri\left[1 + \varepsilon \exp(-\tau/\tau_c)\cos(2\pi y)\right] \tag{9}
$$

where ε = 0.1 and τ_c = 2 are the assumed values. For a given value of the buoyancy parameter, computation is started immediately after the sudden imposition of a uniform wall nondimensional temperature from 0 to 1 on both walls over the finite nondimensional length l_2 at time τ = 0. After an initial transient of approximately τ = 300 nondimenional time units, the value of the Richardson number is varied every $\Delta\tau$ = 100 using a descending step size of ΔRi = 0.2 or ΔRi = 1. The final dynamical state reached by the system is compared against the solution obtained for a given value of the buoyancy parameter prior to the buoyancy drop using the global parameters described above.

NUMERICAL RESULTS

In this section we discuss the hysteresis phenomenon which has been found in the countercurrent mixed convection system described above by varying the value of the buoyancy (Richardson number). The numerical results presented in this work correspond in all cases to a solution without the temporal asymmetric artificial perturbation term of equation (9), except when explicitly mentioned. After switching buoyancy on, the flow reverses close to the heated slabs and two vortices develop. In order to follow the migration of the vortex structure, the value of the stagnation point, X_s is plotted as a function of the nondimensional time.

Fixed value of the buoyancy parameter

First, simulations are carried out for a fixed value of the Richardson number. Figure 2 shows the time evolution of the location of the stagnation point of each vortex for a Richardson number of Ri = 8 [13]. Figure 3 displays the time evolution of the overall Nusselt numbers for a Richardson number of Ri = 8 [13]. By inspecting Figures 2 and 3, simulations demonstrate that for this value of the buoyancy parameter, local vortex oscillations (Hopf bifurcation) takes place.

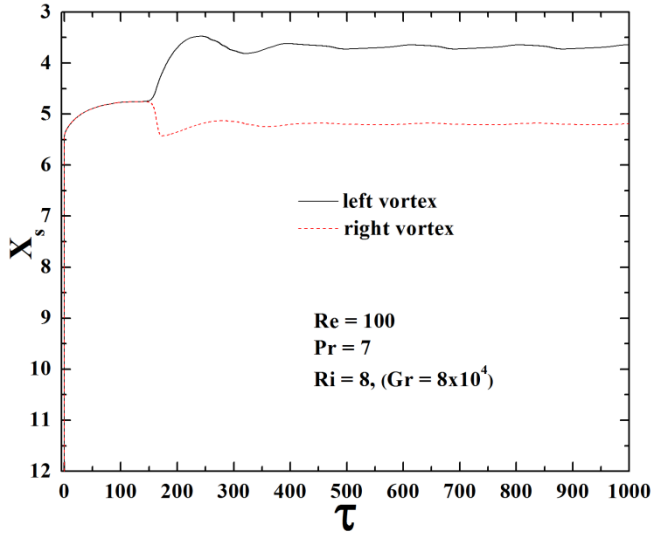

Figure 2 Time evolution for the vortices' upper positions for Ri = 9.

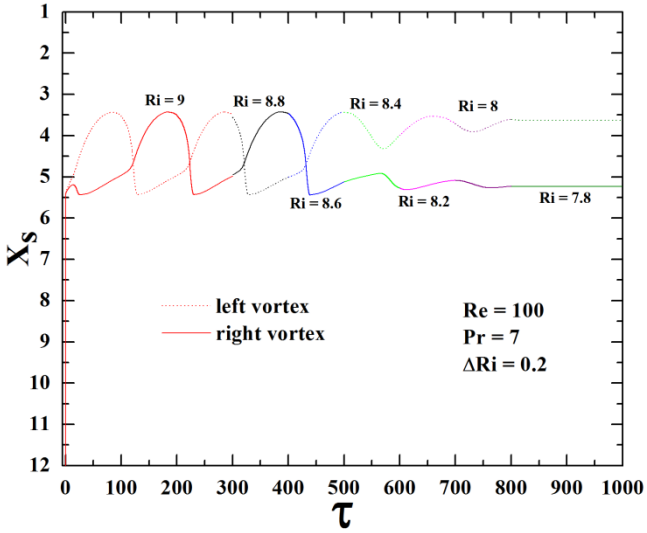

Figure 4 Time evolution for the vortices' upper positions starting at Ri = 9 and imposing decrements of ΔRi = 0.2.

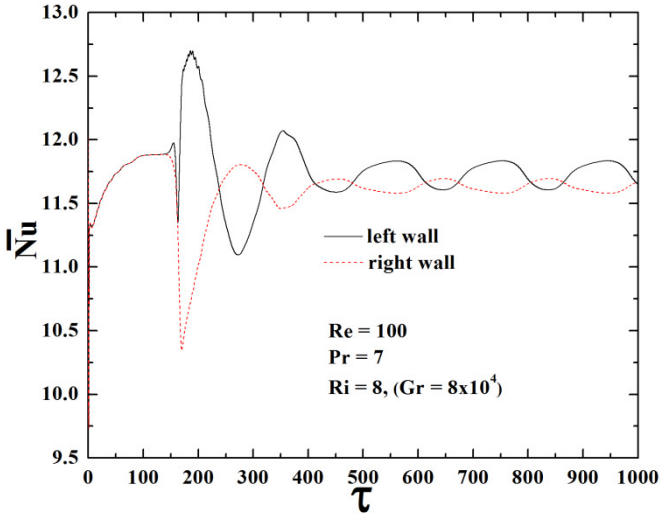

Figure 3 Time evolution for the overall Nusselt numbers for Ri = 9.

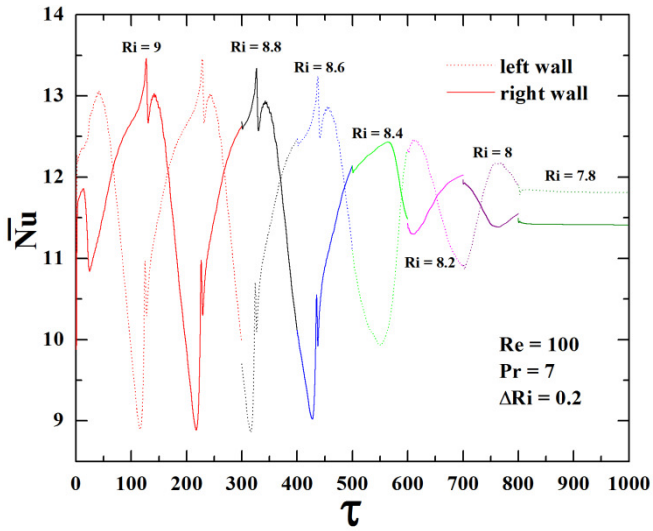

Figure 5 Time evolution for the overall Nusselt numbers starting at Ri = 9 and imposing decrements of ΔRi = 0.2.

Cycling forcing buoyancy

Figure 4 shows the time evolution for the vortices' upper positions for Re = 100, starting with a Richardson number of Ri = 9 and imposed decrements of ΔRi = 0.2. The dotted and continuous lines correspond to the left and right vortex, respectively. For clarity, every time a decrement in the buoyancy parameter takes place, the line colour is changed. The same line and colour pattern is used in Figure 5, which displays the time evolution of the overall Nusselt numbers starting at Ri = 9 and imposed decrements of ΔRi = 0.2. Note how for Ri > 8, the system's final state displays local vortex oscillation, as in Figures 2 and 3. However, when the value of the buoyancy parameter is Ri < 8, transition to a steady asymmetric flow occurs. Hence, no hysteretic behavior occurs for Ri > 8, since the transition to a final steady-state solution proceeds along the same path and is not affected by the decreasing value of the buoyancy.

Figure 6 shows the flow's time history for several values of the Richardson number when increasing and subsequently decreasing the value of the value of the buoyancy. For this case, the modified Richardson number of equation (9) is employed. The nonlinear dynamical response of the system is assessed by inspecting the mean value of the overall Nusselt numbers. For values of the Richardson number smaller than Ri < 5.2 [13], the symmetrical response is stable to infinitesimal perturbations. For larger values the solution losses the symmetry and one of vortices climbs, producing an asymmetrical solution. If now the Richardson number is progressively decreased starting from a point of the asymmetric branches until a final steady-state symmetric response is achieved, buoyancy drop hysteresis is observed. The transition from asymmetric to symmetric steady-state indicates the existence of a subcritical pitchfork bifurcation. Hence, the system is linearly stable but unstable to

a finite perturbation. The hysteretic behavior obtained by cycling the value of the buoyancy is illustrated in Figure 6, where the dotted black line and the continuous red line display the increasing and decreasing paths, respectively. It is interesting to note that the value of the overall Nusselt number has higher values on the descending path of the flow cycle.

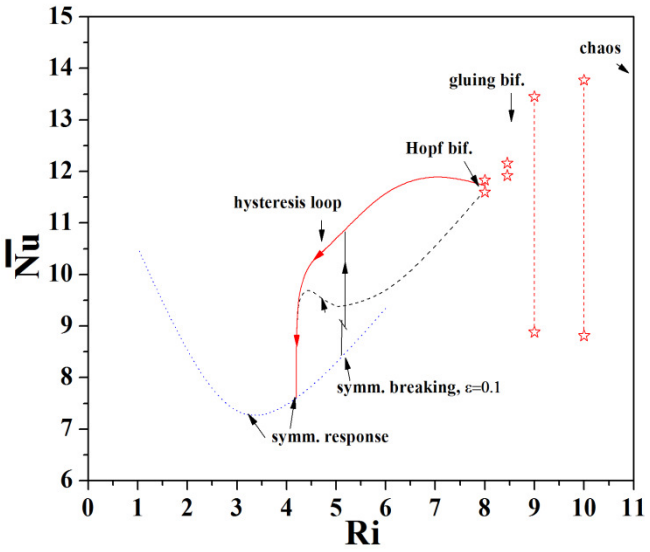

Figure 6 Flow's time history of the mean overall Nusselt number obtained after cycling the forcing buoyancy (Richardson number).

Numerical predictions indicate that no effect on the step size is detected, i.e., stepwise or smooth reductions of the buoyancy parameter to a lower final value did not change the final state achieved.

CONCLUSION

In the present study, numerical simulations have been conducted for a gravity driven two-dimensional mixed convection flow confined in a vertical channel of finite length and heated discretely using isothermal heat sources in order to describe the flow stability and dynamics with respect to an imposed buoyancy drop. As the value of the buoyancy (Richardson number) is varied, different flow regimes are observed, including symmetric and asymmetric steady-states, periodic and chaotic flow. This work deals with quantifying and describing the hysteretic behaviour of the aforementioned system.

In particular, for Re = 100, Pr = 7 and Richardson numbers ranging between 1 and 8, numerical predictions show that variations of the buoyancy over this range give rise to a hysteresis cycle which is characterized by two abrupt transitions between symmetric and asymmetric flow patterns. This behaviour indicates the existence of a subcritical pitchfork (symmetry breaking) bifurcation. Here, the subcritical instability is triggered by a vanishingly small artificial perturbation or modified Richardson number.

The main conclusions are the following: (i) we observe hysteresis in the asymmetrical steady-state regime, such that the transition between different dynamical states proceeds along different paths depending upon the flow's time history, (ii) our findings indicate that the shape and extent of the hysteresis cycle is strongly dependant on the system's initial dynamical state prior to decreasing the value of the buoyancy, and (iii) no effect on the step size has been detected.

ACKNOWLEDGEMENTS

This work has been supported by Grant No. 167474 of Consejo Nacional de Ciencia y Tecnología (CONACyT).

REFERENCES

[1] Bhowmik, H., Tso, C.P., Tou, K.W., and Tan, F.L., Convection heat transfer from discrete heat sources in a liquid cooled rectangular channel, *Applied Thermal Engineering*, Vol. 25, 2005, pp. 2532-2542

[2] Madhusudhana Rao, and G., Narasimham, G.S.V.L., Laminar conjugate mixed convection in a vertical channel with heat generating components, *International Journal of Heat and Mass Transfer*, Vol. 50, 2007, pp. 3561-3574

[3] Watson, J.C., Anand, N.K., and Fletcher, L.S., Mixed convective heat transfer between a series of vertical parallel plates with planar heat sources, *Journal of Heat and Mass Transfer*, Vol. 118, 1996, pp. 984-990

[4] Tsay. Y.L., Transient conjugated mixed-convective heat transfer in a vertical plate channel with one wall heated discretely, *Heat and Mass Transfer*, Vol. 35, No. 5, 1999, pp. 391-400

[5] Aung, W., Mixed Convection in Internal Flow, *Handbook of Single-Phase Convective Heat Transfer*, S. Kakac, R.K. Shah and W. Aung eds. John Wiley and Sons, New York, Chapter 15, 1987

[6] Gebhart, B., Jaluria, Y., Mahajan, R.L., and Sammakia, B., Buoyancy –Induced Flows and Transport, *Hemisphere, Chapter 10, Washington, DC*, 1980

[7] Incropera, F.P., Buoyancy Effects in Double-Diffusive and Mixed Convection Flows, *Proc. 8th Int. Heat Transfer Conference, Washington, DC, Hemisphere Publishing Corp.*, Vol. 1, 1986, pp. 121-130

[8] Habchi, S., and Acharya, S., Laminar mixed convection in a symmetrically or asymmetrically heated vertical channel, *Numerical Heat Transfer, Part A*, Vol. 9, No. 5, 1986, pp. 605-618

[9] Evans, G., Greif, R., Buoyant instabilities in downward flow in a symmetrically heated vertical channel, *International Journal of Heat and Mass Transfer*, Vol. 40, 1997, pp. 2419-2425

[10] Lin, T.-S., Chang, T.-S., and Chen, Y.F., Development of oscillatory asymmetric recirculating flow in transient laminar opposing mixed convection in a symmetrically heated vertical channel, *ASME Journal of Heat Transfer*, Vol. 115, 1993, pp. 342-352

[11] Chang, T.S., and Lin, T.F., Steady and oscillatory opposing mixed convection in a symmetrically heated vertical channel with a low-Prandtl number fluid, *International Journal of Heat and Mass Transfer*, Vol. 35, No. 15, 1993, pp. 3783-3795

[12] Martínez-Suástegui, L., Treviño, C., Particle image velocimetry measurements for opposing flow in a vertical channel with a differential and asymmetric heating condition, *Experimental Thermal and Fluid Science*, Vol. 32, 2007, pp. 262-275

[13] Martínez-Suástegui, L., Treviño, C., and Cajas, J.C., Thermal nonlinear oscillator in mixed convection, *Physical Review E*, Vol. 84, 2011, pp. 046310

[14] Busse, F.H., The stability of finite amplitude cellular convection and its relation to an extremum principle, *Journal of Fluid Mechanics*, Vol. 30, 1967, pp. 625-649
[15] Busse, F.H., Non-linear properties of thermal convetion, *Reports on Progress in Physics*, Vol. 41, 1978, pp. 1929-1967
[16] Vadasz, P., Chaotic dynamics and hysteresis in thermal convection, *Journal of Mechanical Engineering Science*, Vol. 220, 2006, pp. 309-323
[17] Martínez-Suástegui, L., Treviño, C., Transient laminar opposing mixed convection in a differentially and asymmetrically heated vertical channel of finite length, *International Journal of Heat and Mass Transfer*, Vol. 51, 2008, pp. 5991-6005